Supplementary material for

A near-infrared fluorescent probe for detecting Cu^{2+} and its versatile applications

Peijun Li [a], Junjie Yang [b], Liqiang Yan [a, b]*

[a]Guangdong Provincial Key Laboratory of Utilization and Conservation of Food and Medicinal Resources in Northern Region, Shaoguan University, Shaoguan 512005, China

[b]College of Chemistry and Bioengineering, Guilin University of Technology, Guilin 541006, China

*Corresponding author, E-mail: liqiangyan@glut.edu.cn

Table S1. Comparison of the detection performance of some fluorescent probes.

Probe	λ_{ex}	λ_{em}	Stokes shift	Linearity range	LOD	Applications	Ref.
1	615 nm	775 nm	160 nm	0–20 μM	0.0543 μM	SH-SY5Y cells, mouse brain, zebrafish	34
2	375 nm	580 nm	205 nm	0–70 μM	0.25 μM	Water, smartphone, detection kit, HeLa cells, zebrafish	35
3	430 nm	662 nm	232 nm	0–1 μM	1.8 nM	PC12 cells, zebrafish, mouse	36
4	350 nm	439 nm	89 nm	0–80 μM	0.0565 μM	BHK-21 cells	37
5	405 nm	515 nm	110 nm	0–20 μM	0.6 μM	Raw264.7 cells	38
6	520 nm	663 nm	143 nm	0–10 μM	0.13 μM	Water, Hela cells	39
7	470 nm	585 nm	115 nm	4–10 μM and 10–35 μM	82.6 nM and 409.7 nM	MCF-7 cells, test paper	40
8	400 nm	510 nm	110 nm	0–6 μM	0.0416 μM	Water, test paper, HepG2 cells	41
9	385 nm	495 nm	110 nm	0–10 μM	0.62 μM	Aqueous media	42
10	420 nm	655 nm	235 nm	0–100 μM	0.018 μM	Water, food (rice, mung beans), plant (onion roots), soil, test strips, smartphone	this work

S1 Reagents and instruments

All anions were derived from their corresponding sodium salts. All cations were obtained in the form of nitrate salts. All solvents, unless otherwise specified, are commercially available and analytically pure.

Nuclear magnetic date (^{1}H and ^{13}C NMR) was measured at room temperature with TMS as the internal standard (Bruker Avance III Ascend, 500 MHz). Ultraviolet-visible spectra were tested with PerkinElmer Lambda 750 ultraviolet spectrophotometer. Fluorescence spectra were measured with F98 fluorescence spectrophotometer (Shanghai Lengguang Technology Co., Ltd., China). Mass spectrometry analyses were performed using an Agilent 6400 series triple quadrupole mass analyzer. Plant tissue imaging was conducted with an Olympus IX53 inverted fluorescence microscope, with images captured in three spectral channels under 400 nm excitation: blue (420 – 500 nm), green (500 – 565 nm), and red (565 – 650 nm) emission ranges.

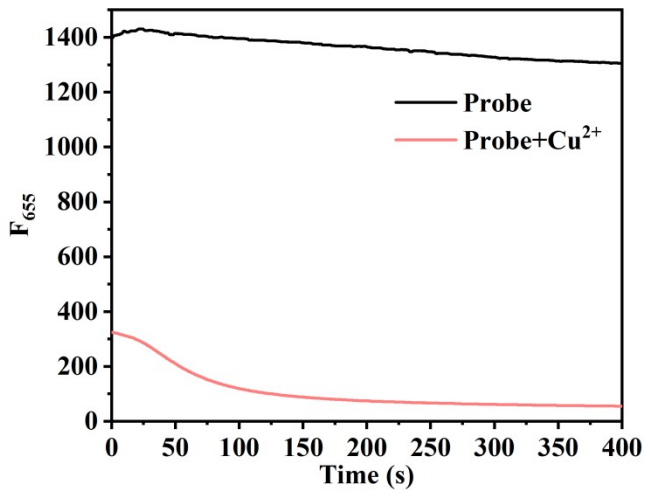

Fig. S1. The trend of fluorescence intensity at 655 nm of the probe DCPO-Cu with time after adding Cu^{2+}.

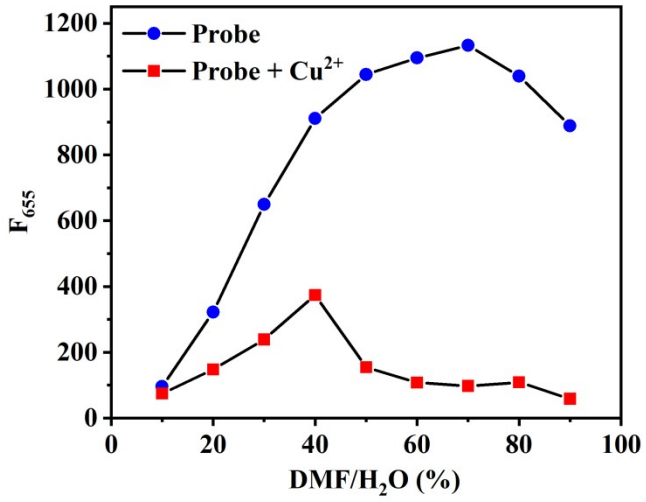

Fig. S2. The fluorescence intensity at 655 nm of the probe DCPO-Cu changed with the composition of solvent after the addition of Cu^{2+}.

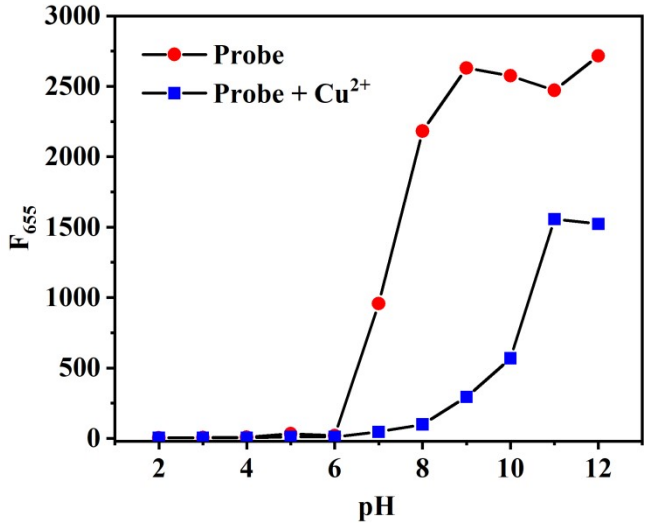

Fig. S3. Fluorescence intensity at 655 nm of the probe DCPO-Cu changed with the pH of the solution after adding Cu^{2+}.

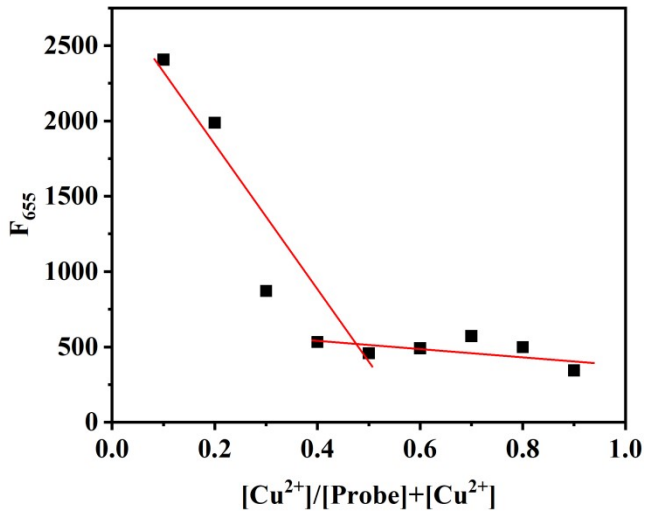

Fig. S4. Job's plot between the probe DCPO-Cu and Cu^{2+}.

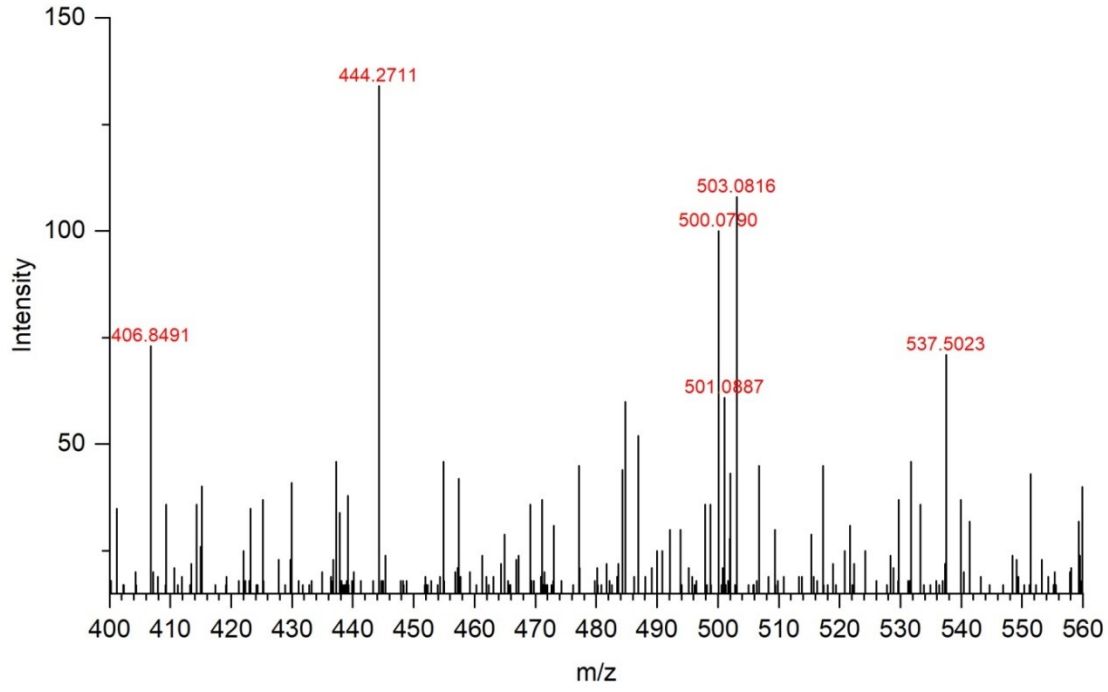

Fig. S5. HR-MS of the probe DCPO-Cu after reaction with Cu^{2+}.

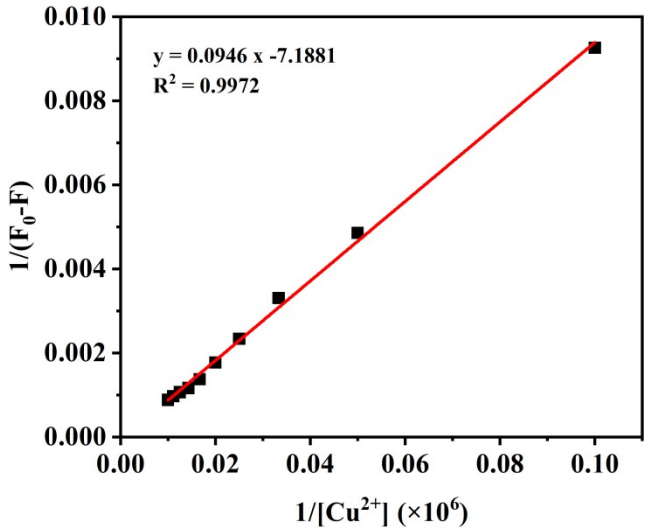

Fig. S6. Benesi-Hildebrand linearity between the probe DCPO-Cu and Cu^{2+}.

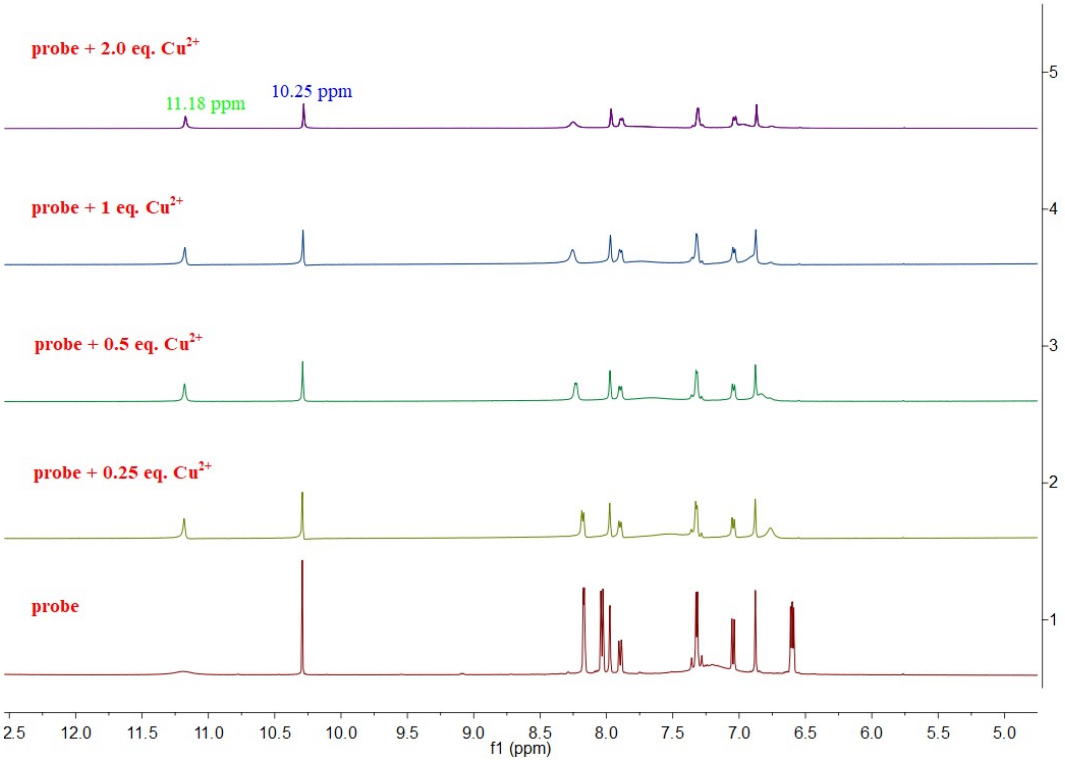

Fig. S7. ^{1}H NMR spectra of the probe DCPO-Cu before and after adding Cu^{2+}.

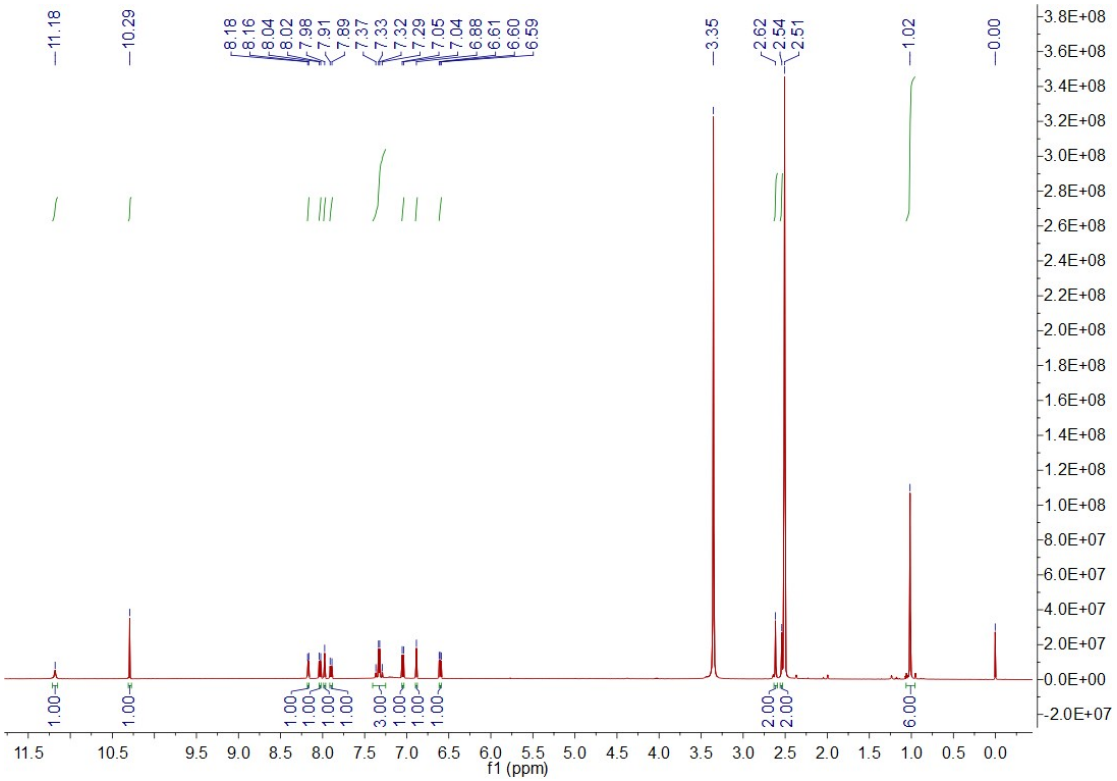

Fig. S8. ^{1}H NMR of the probe DCPO-Cu.

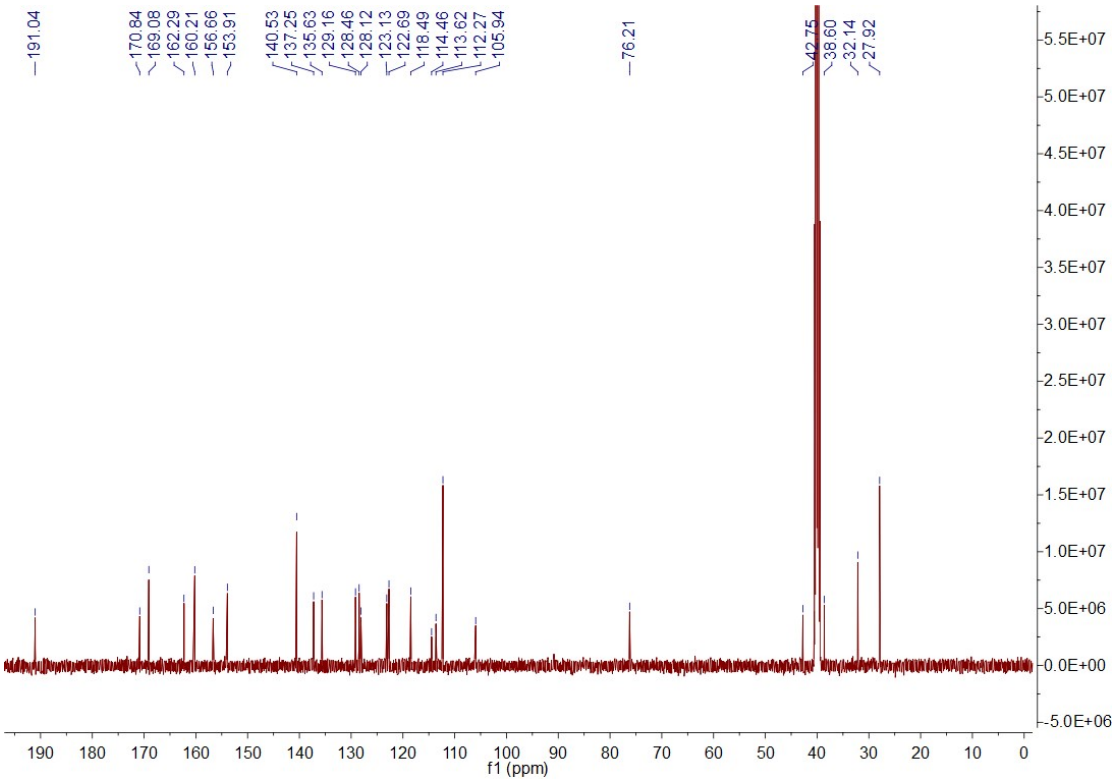

Fig. S9. ^{13}C NMR of the probe DCPO-Cu.

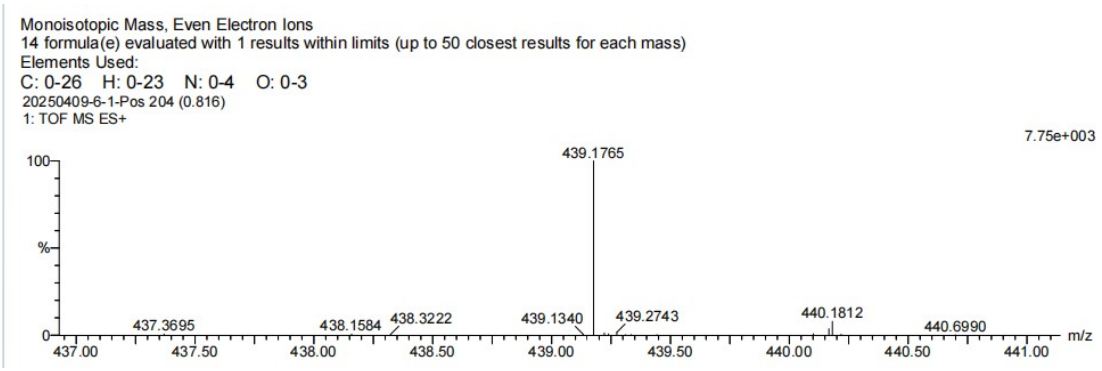

Fig. S10. HR-MS of the probe DCPO-Cu.